Modulation of the aspartic acid scaffold to identify a new septin-4 covalent binder with anti-metastatic activity in a mouse model of melanoma

F. Boccato,[a] F. Blua,[a] A. A. Altomare,[b] S. Vittorio,[b] N. Clemente,[c] C. Monge,[a] E. Marini,[a] M. Bertinaria.[a]

[a] *Department of Drug Science and Technology, University of Turin, Italy*
[b] *Department of Pharmaceutical Sciences, University of Milan, Italy*
[c] *Settore Centri di Ricerca e Infrastrutture, University of Piemonte Orientale, Novara, Italy*
francesca.boccato@unito.it

Structural modulations of compound AA6

Since compound AA6, previously synthesised by our research group, is able to prevent metastasis formation in the 4T1 mouse model of breast cancer[1], structural modulations were performed in order to find the structural determinants of the anti-metastatic effect and to identify the cellular target.[2]

Modulations performed:

- R_1, R_2, R_3: Aspartic acid moiety
- R_4: distance between the benzene ring and the amide group
- R_5: steric hindrance

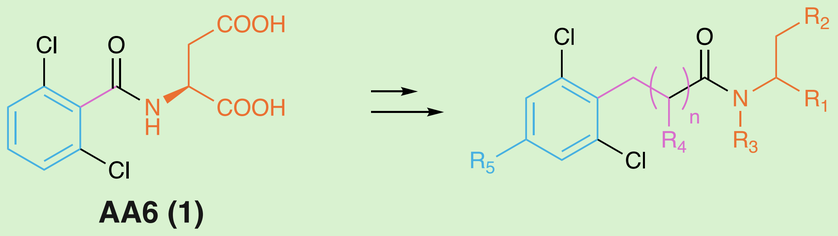

AA6 (1)

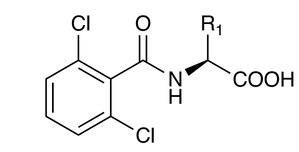

R_1

2 $CH_2CH(CH_3)_2$
3 CH_2-4-imidazolyl
4 $CH_2CH_2NHC(NH)NH_2$
5 CH_2CONH_2

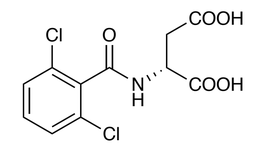

6

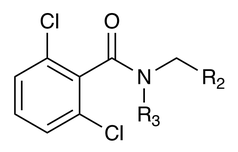

	R_2	R_3
7	COOH	H
8	COOH	CH_3
9	CH_2COOH	H

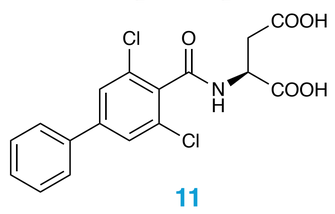

11

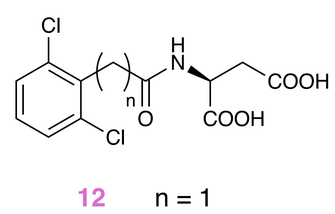

12 n = 1
13 n = 2

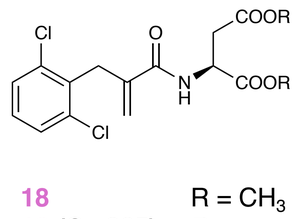

18	$R = CH_3$
19 (CM365)	R = H

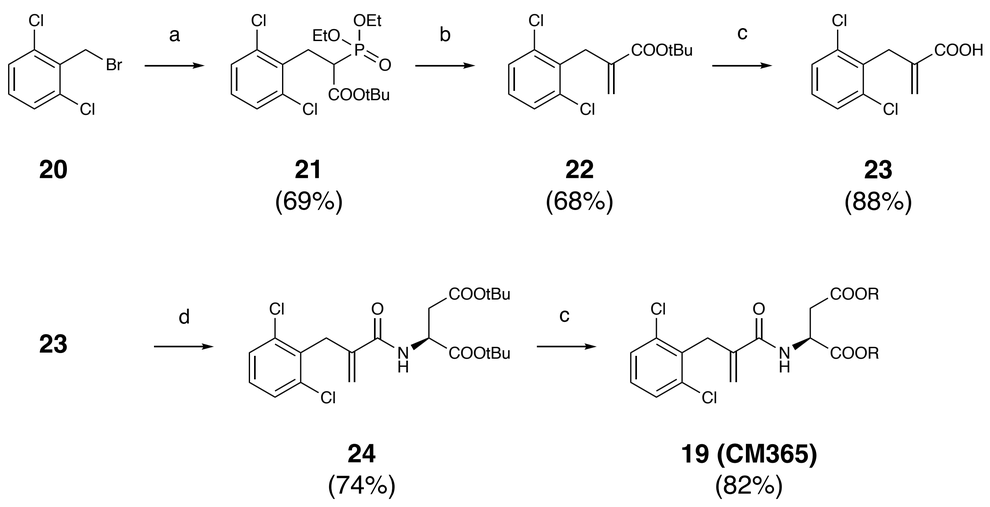

20

21 (69%)

22 (68%)

23 (88%)

24 (74%)

19 (CM365) (82%)

Scheme 1. *Reagents and conditions: (a) tert-butyl diethylphosphonoacetate (1.2 eq), NaH (1.4 eq), DMF, rt, 2 h. (b) paraformaldehyde (8 eq), K_2CO_3 (3 eq), water, 90 °C, 72 h. (c) TFA/DCM (10 %), rt, 18 h. (d) L-aspartic acid di-tert-butyl ester (1.1 eq), HBTU (1.5 eq), HOBt (0.1 eq), DIPEA (3 eq), DMF, 18 h.*

In vitro lead compound selection and its synthesis

Compound	Maximal efficacy [a] % inhibition at 100 µM ± SE	IC_{50} (µM) ± SE [b]
1 (AA6)	70 ± 4	0.7 ± 0.1
2	29 ± 2	nc[c]
3	42 ± 1	nc[c]
4	52 ± 2	45 ± 9
5	65 ± 5	0.7 ± 0.4
6	Not active	nc[c]
7	45 ± 3	nc[c]
8	39 ± 2	nc[c]
9	41 ± 1	nc[c]
11	35 ± 2	nc[c]
12	55 ± 5	4.5 ± 3
13	60 ± 4	2.4 ± 1
18	Not active	nc[c]
19 (CM365)	56 ± 7	5.5 ± 3.8

Table 1. Inhibition of B16-F10 cells invasion. [a] Percentage inhibition of B16-F10 cells invasiveness at the maximal concentration tested (100 µM) versus control invasion measured on untreated cells. [b] IC_{50} values calculated for the most active compounds (maximal efficacy at 100 µM > 50 %). [c] Not calculated.

The synthesised compounds were tested for their ability to inhibit invasiveness of B16-F10 melanoma cells. The modulation of the aspartic acid moiety (2-9) significantly decreases the maximal efficacy, except for the amide compound 5, with respect to AA6. Compound 6 was found inactive, so the *S* configuration of the chiral carbon seems to be essential. The insertion of a phenyl ring in compound 11 causes loss of activity. The insertion of the spacer (12-13) did not significantly affect the activity. Thus, we synthesised compound 19 with an activated double bond able to form covalent Michael-type adducts. CM365 maintained a good maximal efficacy with a higher IC_{50} compared to AA6, while its dimethyl ester analogue 18 was inactive. For these reasons **CM365** was selected for later studies.

Target identification

As a Michael acceptor, CM365 could form stable adduct with the target, that can be detected by a proteomic analysis. Previously we discovered that the compound is not able to penetrate the cell membrane, thus we proceeded identifying the adduct(s) by nLC-HR-MS/MS. B16-F10 cells were first incubated with the inhibitor and then the membrane fractions isolated were analysed. We processed the experimental MS spectra searching selectively for mass shifts generated by adducts with nucleophilic aminoacids (*Fig. 1A*). Then, an automatic matching tasks (*Proteome Discoverer* software) was used to assign the peptide adduct within a theoretical list of the most plausible PSMs (peptide spectral matches, *Fig. 1C*). After a manual evaluation of the reports, we identified the formation of one stable conjugate among CM365 and the residue Lys290 of the protein **Septin-4** (*Fig. 1B*).

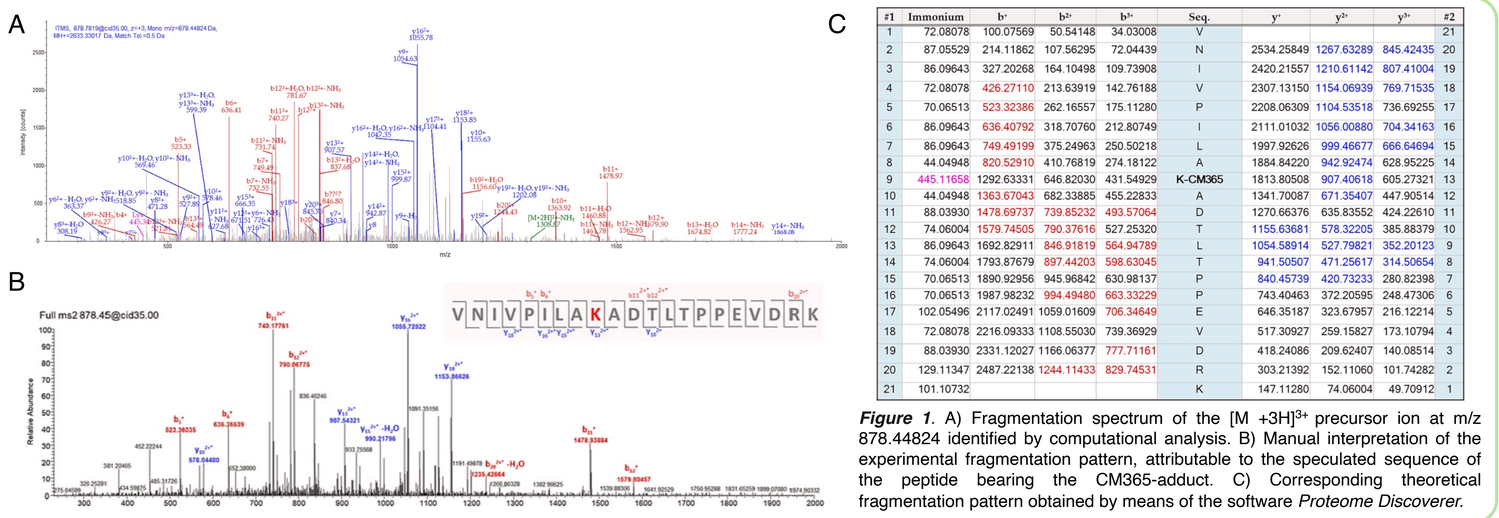

#1	Immonium	b^+	b^{2+}	b^{3+}	Seq.	y^+	y^{2+}	y^{3+}	#2
1	72.08078	100.07569	50.54148	34.03008	V				21
2	87.05529	214.11862	107.56295	72.04439	N	2534.25849	1267.63289	845.42435	20
3	86.09643	327.20268	164.10498	109.73908	I	2420.21557	1210.61142	807.41004	19
4	72.08078	426.27110	213.63919	142.76188	V	2307.13150	1154.06939	769.71535	18
5	70.06513	523.32386	262.16557	175.11280	P	2208.06309	1104.53518	736.69255	17
6	86.09643	636.40792	318.70760	212.80749	I	2111.01032	1056.00880	704.34163	16
7	86.09643	749.49199	375.24963	250.50218	L	1997.92626	999.46677	666.64694	15
8	44.04948	820.52910	410.76819	274.18122	A	1884.84220	942.92474	628.95225	14
9	445.11658	1292.63331	646.82030	431.54929	K-CM365	1813.80508	907.40618	605.27321	13
10	44.04948	1363.67043	682.33885	455.22833	A	1341.70087	671.35407	447.90514	12
11	88.03930	1478.69737	739.85232	493.57064	D	1270.66376	635.83552	424.22610	11
12	74.06004	1579.74505	790.37616	527.25320	T	1155.63681	578.32205	385.88379	10
13	86.09643	1692.82911	846.91819	564.94789	L	1054.58914	527.79821	352.20123	9
14	74.06004	1793.87679	897.44203	598.63045	T	941.50507	471.25617	314.50654	8
15	70.06513	1890.92956	945.96842	630.98137	P	840.45739	420.73233	280.82398	7
16	70.06513	1987.98232	994.49480	663.33229	P	743.40463	372.20595	248.47306	6
17	102.05496	2117.02491	1059.01609	706.34649	E	646.35187	323.67957	216.12214	5
18	72.08078	2216.09333	1108.55030	739.36929	V	517.30927	259.15827	173.10794	4
19	88.03930	2331.12027	1166.06377	777.71161	D	418.24086	209.62407	140.08514	3
20	129.11347	2487.22138	1244.11433	829.74531	R	303.21392	152.11060	101.74282	2
21	101.10732				K	147.11280	74.06004	49.70912	1

Figure 1. A) Fragmentation spectrum of the $[M + 3H]^{3+}$ precursor ion at m/z 878.44824 identified by computational analysis. B) Manual interpretation of the experimental fragmentation pattern, attributable to the speculated sequence of the peptide bearing the CM365-adduct. C) Corresponding theoretical fragmentation pattern obtained by means of the software *Proteome Discoverer.*

Computational studies

After obtaining SEP4-SEP6 complex by homology modelling, it was used to perform docking studies of compounds AA6 and CM365 (using GOLD v2020.1 software, *Fig. 2A,B*). The simulations highlighted that the carboxyl group is involved in H-bonds with G156, S158 of SEP4 for both compounds, while AA6 also forms additional interactions with T159 and R173. Notably, CM365 is able to bind covalently to K290. Moreover, the effect of this covalent adduct formation on the stability of the SEP4-SEP6 complex was explored by performing MD simulations (using AMBER 18 software, *Fig. 2C*). Specifically, CM365 induces multiple structural changes at the interface between the two proteins, represented by the *trans*-loop I of SEP4 (around residue 329, *Fig. 2D*) and the switch I region of SEP6 (residues 69-77, *Fig. 2E*), variations that may be responsible for SEP4 inhibition.

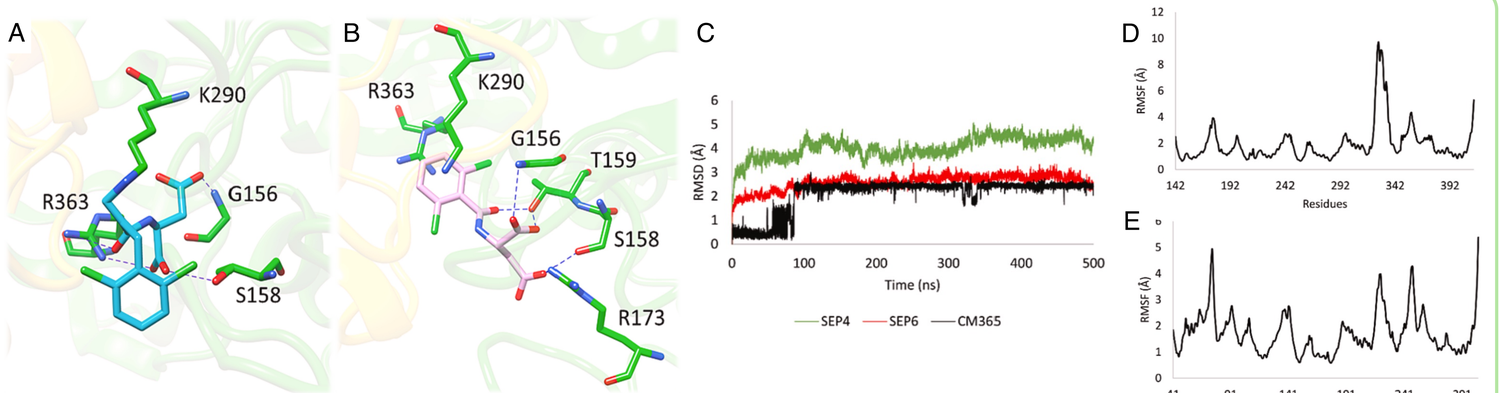

Figure 2. Docking poses of A) CM365, B) AA6 performed on the homology model of SEP4(green)-SEP6(yellow) dimer. The residues involved are depicted as sticks, H-bonds as blue dashed lines. C) RMSD plot of CM365 and SEP4-SEP6 backbone. D) RMSF profile of SEP4. E) RMSF profile of SEP6.

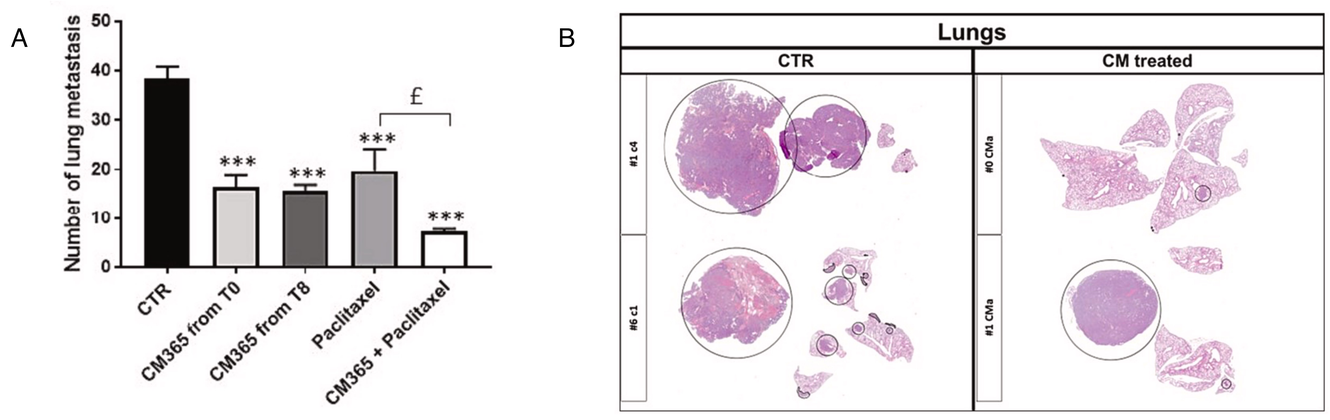

Figure 3. In vivo inhibition of lung metastasis dissemination. A) number of lung metastasis in untreated (CTR: vehicle only i.p. for 20 days) and treated mice: CM365 12.5 mg/kg i.p. from day 0 (T0), CM365 12.5 mg/kg i.p. from day 8 (T8), paclitaxel 5 mg/kg i.v. on day 7, and CM365 (T0) +paclitaxel (T7); *** P <0.0001 vs CTR; £P < 0.05 CM365 +paclitaxel vs paclitaxel, One-way ANOVA Bonferroni Multiple Comparisons Test. Data are expressed as mean ±SEM (n ≥5). B) Hematoxylin eosin staining of lung tumor tissue sections belonging to two representative animals (left: CTR group, right: CM365 treated group); spreading metastasis are pinpointed with black circles.

In vivo studies of lung metastasis mouse model of melanoma

The antimetastatic activity of CM365 was also evaluated *in vivo* in a mouse model of metastatic melanoma using B16-F10 cells evaluating the occurrence of lung metastases.[3] CM365 treatment significantly reduced metastasis dissemination when administered at T0 and T8. Its effect was increased by co-administration of paclitaxel, a well-known chemotherapeutic agent (*Fig. 3A*). Histological examination of the lung-stained sections confirmed the antimetastatic effect of CM365 compared to the control (*Fig. 3B*).

References

[1] Atlante, S. et al. α-ketoglutarate dehydrogenase inhibition counteracts breast cancer-associated lung metastasis. Cell Death Dis 9, 756 (2018).
[2] Blua, F. et al. Discovery of a septin-4 covalent binder with antimetastatic activity in a mouse model of melanoma, Bio Chem, 144 (2024).
[3] W.W. Overwijk, N.P. Restifo, B16 as a mouse model for human melanoma. Curr Protoc Immunol. 2001, Chapter 20: Unit 20.1.

UNIVERSITÀ DI TORINO
UPO UNIVERSITÀ DEL PIEMONTE ORIENTALE
UNIVERSITÀ DEGLI STUDI DI MILANO